Supplementary Tables

Case	Diagnosis	Tissue	WHO grade	%CA9	%CDH22	%CA9 coloc. with CDH22	%CDH22 coloc. with CA9
1	Astrocytoma	Tumor	III	3.6	3.8	91.2	90.6
2	Astrocytoma	Tumor	III	3.5	4.2	91.4	87.1
3	Astrocytoma	Tumor	III	6.5	8.6	93.9	83.8
4	Oligodendroglioma	Tumor	III	6.5	5.2	86.8	82.9
5	Oligodendroglioma	Tumor	III	3.0	4.9	82.7	94.5
6	Oligodendroglioma	Tumor	III	45.2	43.8	94.8	96.3
7	Oligodendroglioma	Tumor	III	20.6	16.1	83.5	92.0
8	Oligodendroglioma	Tumor	III	4.0	2.8	76.2	73.2
9	Oligoastrocytoma	Tumor	III	16.0	19.4	98.2	86.7
10	Oligodendroglioma	Tumor	III	19.2	20.7	98.9	95.4
10		Normal	-	3.3	3.3	100	100
11	Oligodendroglioma	Tumor	III	18.8	19.2	95.4	93.8
12	Oligodendroglioma	Tumor	III	7.6	8.9	90.4	85.2
13	Oligidendroglioma	Tumor	III	13.7	15.9	90.3	87.2
14	Glioma – anaplastic	Tumor	III	4.5	3.0	76	83.6
14		Normal	-	3.0	3.0	100	100
15	Diffuse glioma	Tumor	III	6.5	5.6	86.4	88.3
16	Glioma – anaplastic	Tumor	III	7.2	7.0	88.4	84.0
17	Oligodendroglioma	Tumor	III	15.6	16.2	91.7	86.0
18	Astrocytoma	Tumor	III	5.5	5.9	95.5	92.8
19	Astrocytoma	Tumor	III	9.7	10.1	93.3	88.5
20	Astrocytoma	Tumor	III	9.3	9.0	94.1	95.2
21	Glioblastoma	Tumor	IV	24.8	38.1	93.6	72.3
22	Glioblastoma	Tumor	IV	28.6	38.7	90.7	74.3
23	Glioblastoma	Tumor	IV	30.5	42.9	87.9	76.7
24	Glioblastoma	Tumor	IV	37.2	33.3	85.7	92.9
25	Glioblastoma	Tumor	IV	33.8	42.8	92.5	83.9
26	Glioblastoma	Tumor	IV	22.0	25.1	91.9	86.4
27	Glioblastoma	Tumor	IV	40.7	52.8	95.0	85.4
28	Glioblastoma	Tumor	IV	38.0	50.3	90.7	76.7
29	Glioblastoma	Tumor	IV	36.1	50.5	95.5	80.9
30	Glioblastoma	Tumor	IV	20.4	23.6	90.1	77.7
31	Glioblastoma	Tumor	IV	33.2	39.6	91.7	81.8
32	Glioblastoma	Tumor	IV	30.9	42.5	95.4	74.0
33	Glioblastoma	Tumor	IV	25.4	32.8	95.8	82.9
34	Glioblastoma	Tumor	IV	28.1	39.0	92.0	85.9
35	Glioblastoma	Tumor	IV	26.5	40.4	96.2	75.2
36	Glioblastoma	Tumor	IV	29.8	37.4	95.1	88.8
37	Glioblastoma	Tumor	IV	34.6	46.8	98.0	78.2
38	Glioblastoma	Tumor	IV	29.0	25.3	91.8	95.2

39	Glioblastoma	Tumor	IV	23.2	21.9	95.7	97.4
40	Glioblastoma	Tumor	IV	31.7	40.8	99.2	78.2
41	Glioblastoma	Normal	-	3.5	3.5	100	100
42	Glioblastoma	Normal	-	4.2	4.2	100	100
43	Metastasis - breast	Normal	-	5.5	6.0	100	86.6
44	Oligodendroglioma	Normal	-	2.3	2.3	100	100
45	Glioblastoma	Normal	-	3.5	4.5	100	82.5
46	Oligodendroglioma	Normal	-	2.3	3.5	100	87.5
47	Oligodendroglioma	Normal	-	1.5	1.5	100	100
48	Glioblastoma	Normal	-	0.5	0.5	100	100
Avg. Grade III				**11.3 ± 2.2**	**11.5 ± 2.2**	**90.0 ± 1.4**	**88.4 ± 1.3**
Avg. Grade IV				**30.2 ± 1.2**	**38.2 ± 2.0**	**93.2 ± 0.7**	**82.2 ± 1.6**
Avg. Normal				**3.0 ± 0.4**	**3.2 ± 0.5**	**100**	**95.7 ± 2.2**

Supplementary Table 1. Quantification of carbonic anhydrase 9 (CA9) and cadherin-22 (CDH22) expression and colocalization in 40 cases of human glioma and 10 of normal adjacent brain tissue. Twenty high grade tumors (glioblastoma; WHO grade IV) and twenty lower grade anaplastic gliomas (WHO grade III) were analyzed along with 10 normal brain tissue samples. Due to the availability of specimens, there were only two instances where tumor and normal adjacent samples could be taken from the same patient (patients 10 and 14). The other eight normal samples were taken from patients where a corresponding tumor sample was not available. Hypoxia (CA9) and CDH22 expression was quantified using ImageJ by calculating the percent positive pixels (a signal intensity above the set threshold of 2.5-fold greater than background). Colocalization analyses were performed using Coloc2 in the Fiji plugin for ImageJ to calculate the fractional overlap between CA9 and CDH22 using Manders' Colocalization Coefficients and the Costes method for estimating thresholds above background. Two to four fields of view were imaged and analyzed per tumor sample depending on the size of

the section. All specimens were taken from the tumor center. Averages represented as means ± s.e.m. WHO, World Health Organization.

Case	Tissue	Stage	Tumor Size (cm)	%CA9	%CDH22	%CA9 colocalization with CDH22	%CDH22 colocalization with CA9
1	Tumor	II	2.8	9.3	17.0	90.5	83.2
2	Tumor	II	3.2	10.8	13.2	94.7	90.0
3	Tumor	II	3.7	12.8	13.7	96.1	93.0
4	Tumor	II	4.0	9.1	11.9	91.6	86.8
5	Tumor	II	3.4	6.8	7.5	89.9	85.1
6	Tumor	II	2.2	11.2	6.5	97.4	99.7
7	Tumor	II	2.5	7.0	7.2	97.2	94.2
8	Tumor	II	3.3	7.8	8.5	87.8	84.9
9	Tumor	II	3.3	12.2	6.8	98.5	96.8
10	Tumor	II	3.7	12.0	16.6	88.8	83.7
11	Tumor	II	3.2	6.2	9.8	94.5	88.2
12	Tumor	II	2.4	7.7	8.9	95.1	89.2
13	Tumor	II	4.0	6.7	9.0	90.0	86.2
14	Tumor	II	4.0	10.9	11.5	96.3	90.4
14	Normal	-	-	1.5	1.5	100	100
15	Tumor	II	3.5	7.3	12.5	96.9	83.4
15	Normal	-	-	2.3	2.3	100	100
16	Tumor	II	2.5	11.8	14.0	100	89.9
16	Normal	-	-	2.0	4.4	93.1	85.9
17	Tumor	II	2.9	9.8	12.9	90.7	85.6
17	Normal	-	-	1.5	1.5	100	100
18	Tumor	II	4.9	10.6	12.0	97.3	94.2
18	Normal	-	-	3.2	4.5	93.9	81.1
19	Tumor	II	4.0	7.5	10.0	91.5	85.5
20	Tumor	III	4.2	27.0	31.3	94.8	87.5
21	Tumor	III	6.5	23.8	23.4	92.3	85.5
22	Tumor	III	7.5	24.2	33.3	84.9	71.6
23	Tumor	III	3.5	17.0	18.7	87.0	78.5
24	Tumor	III	8.5	26.8	27.5	93.8	87.1
25	Tumor	III	6.0	18.4	24.0	93.1	76.9
26	Tumor	III	6.6	21.2	27.4	88.5	76.9
27	Tumor	III	7.0	28.4	33.4	91.8	86.1
28	Tumor	III	8.0	26.1	29.5	93.6	86.3
29	Tumor	III	5.1	24.7	32.8	96.8	81.9
29	Normal	-	-	2.4	4.4	94.1	90.8
30	Tumor	III	3.3	24.8	29.1	93.2	84.9
31	Tumor	IV	5.5	40.4	42.8	87.0	76.0
32	Tumor	IV	5.5	35.2	38.9	95.0	89.3

32	Normal	-	-	1.3	1.3	100	100
33	Tumor	IV	2.5	38.7	39.0	97.8	85.1
34	Tumor	IV	2.1	48.2	50.4	94.9	87.3
35	Tumor	IV	6.0	42.9	39.4	85.2	77.7
36	Tumor	IV	7.0	38.9	58.5	89.2	81.1
36	Normal	-	-	1.5	1.5	100	100
37	Tumor	IV	6.5	48.2	32.3	82.1	94.6
37	Normal	-	-	2.5	2.5	100	100
38	Tumor	IV	7.0	45.2	38.6	95.6	79.2
39	Tumor	IV	13.0	46.1	46.1	99.0	91.2
39	Normal	-	-	3.0	3.0	100	100
40	Tumor	IV	3.5	38.7	55.4	86.5	77.5
Avg. Stage II				**9.3 ± 0.5**	**11.0 ± 0.7**	**93.9 ± 0.8**	**89.0 ± 1.1**
Avg. Stage III				**23.9 ± 1.1**	**28.2 ± 1.4**	**92.0 ± 1.0**	**82.8 ± 1.7**
Avg. Stage IV				**42.3 ± 1.4**	**44.1 ± 2.6**	**91.2 ± 1.9**	**83.9 ± 2.1**
Avg. Normal				**2.1 ± 0.2**	**2.7 ± 0.4**	**98.1 ± 1.0**	**95.8 ± 2.3**

Supplementary Table 2. Quantification of carbonic anhydrase 9 (CA9) and cadherin-22 (CDH22) expression and colocalization in 40 cases of human invasive ductal breast carcinoma and 10 of normal adjacent tissue. Forty invasive ductal breast carcinoma cases (19 stage II, 11 stage III, and 10 stage IV) were analyzed along with 10 normal adjacent tissue samples. Hypoxia (CA9) and CDH22 expression was quantified using ImageJ by calculating the percent positive pixels (a signal intensity above the set threshold of 2.5-fold greater than background). Colocalization analyses were performed using Coloc2 in the Fiji plugin for ImageJ to calculate the fractional overlap between CA9 and CDH22 using Manders' Colocalization Coefficients and the Costes method for estimating thresholds above background. Two to four fields of view were imaged and analyzed per tumor sample depending on the size of the section. Tumors were staged via the TNM system. Averages represented as means ± s.e.m.

Supplementary Figure Legend

Supplementary Figure 1. eIF4E2 is required for U87MG cell migration, invasion, and spheroid formation in hypoxia. (**A**) Western blot of eIF4E2 protein levels in control (Ctrl) cells stably expressing a non-targeting shRNA or in cells stably expressing shRNA targeting *eIF4E2* mRNA (KD1.1). GAPDH used as a loading control. (**B**) Control and eIF4E2 KD cells exposed to normoxia (21% O_2) or hypoxia (1% O_2) for 24 h followed by wound generation. Representative images at 0 h (T0) and 12 h (T12) after wound generation. (**C-D**) Transwell migration (**C**) and invasion (**D**) assays of control and eIF4E2 KD cells exposed to normoxia or hypoxia for 24 h. Representative images of trans-well inserts 4 h after seeding and stained with crystal violet. Data are presented relative to normoxic Ctrl as mean ± s.e.m, $n \geq 3$, **P<0.01, ***P<0.001, using a one-way ANOVA followed by Tukey's HSD test. Scale bar, 100 μm.

Supplementary Figure 2. Proliferation and apoptosis rates of MDA-MB-231 and U87MG stable cells lines used in Figures 1-4. (**A-B**) The proliferation rates measured by percent BrdU incorporation (**A**) and apoptosis rates measured by percent cells positive for active capsapse-3 (**B**) in normoxia (21% O_2) and hypoxia (1% O_2) of control (Ctrl) cells stably expressing a non-targeting shRNA, one of two shRNAs targeting *eIF4E2* mRNA: Knockdown (KD) 1 and KD2, and eIF4E2 knockdown control (KD Ctrl) cells stably expressing shRNA targeting *eIF4E2* mRNA and an exogenous empty vector or the *eIF4E2* coding sequence (Exo1 4E2 and Exo2 4E2). Data are presented as mean ± s.e.m of at least three biological replicates.

Supplementary Figure 3. Reintroduction of exogenous eIF4E2 restores the ability of U87MG cells to migrate, invade and adhere to one another in hypoxia. (**A**) Western blot of

eIF4E2 protein levels in control (Ctrl) cells stably expressing a non-targeting shRNA, eIF4E2 knockdown control (KD Ctrl) cells stably expressing shRNA targeting *eIF4E2* mRNA and an exogenous empty vector or the *eIF4E2* coding sequence (Exo1 4E2 and Exo2 4E2). GAPDH was used as a loading control. (**B**) KD Ctrl, Exo1 4E2 and Exo2 4E2 cells exposed to hypoxia (1% O_2) for 24 h followed by wound generation. Representative images at 0 h (T0) and 12 h (T12) after wound generation. (**C-D**) Transwell migration (**C**) and invasion (**D**) assays of KD Ctrl, Exo1 4E2 and Exo2 4E2 cells exposed to hypoxia for 24 h. Representative images of trans-well inserts 4 h after seeding and stained with crystal violet. (**E**) Light micrographs of spheroids composed of KD Ctrl, Exo1 4E2 and Exo2 4E2 cells. Data are presented as mean ± s.e.m, n≥3, ***P<0.001, using a one-way ANOVA followed by Tukey's HSD test. Scale bar, 100 μm.

Supplementary Figure 4. Hypoxia and exogenous expression of CDH22 allow for the detection of CDH22 by immunofluorescence. Immunofluorescence of CDH22 in MDA-MB-231 and U87MG control cells stably expressing a non-targeting shRNA (CDH22 Ctrl), in cells stably expressing shRNA targeting *CDH22* mRNA (KD 3.1), KD cells stably expressing an exogenous *CDH22* coding sequence (Exo1 CDH22) exposed to normoxia (21% O_2) and hypoxia (1% O_2). KD, knockdown. Scale bar, 10 μm. These are controls for Figure 3g.

Supplementary Figure 5. Hypoxia represses *CDH1* mRNA translation and activates CDH22 synthesis in an eIF4E2-dependent manner. (**A-C**) The polysomal association of *CDH1* and *CDH22* mRNAs was observed by RT-PCR in parental (**A**), control cells stably expressing a non-targeting shRNA (**B**), or shRNA targeting *eIF4E2* mRNA (KD 1.1) (**B**), KD cells stably expressing an exogenous empty vector (KD Ctrl) (**C**), or the exogenous *eIF4E2*

coding sequence (Exo1 4E2) (**C**) under the indicated oxygen conditions. (**D**) The polysomal association of *CDH1* and *CDH22* mRNAs was observed by RT-PCR in parental cells exposed to hypoxia and the mTORC1 inhibitor Torin 1 for 2 h. Images are representative of at least three biological replicates. All experiments performed in U87MG glioblastoma.

Supplementary Figure 6. Blocking CDH22 impairs hypoxic U87MG cell migration, invasion, and spheroid formation. (**A**) Parental cells incubated with a control non-targeting antibody (IgG) or an antibody targeting the extracellular domain of CDH22 were exposed to normoxia (21% O_2) or hypoxia (1% O_2) for 24 h followed by wound generation. Representative images at 0 h (T0) and 12 h (T12) after wound generation. (**B-C**) Transwell migration (**C**) and invasion (**D**) assays of parental cells incubated with control or anti-CDH22 antibodies and exposed to normoxia or hypoxia for 24 h. Representative images 12 h after seeding and stained with crystal violet. (**D**) Light micrographs of spheroids composed of parental cells incubated with control or anti-CDH22 antibodies. Data are presented as mean ± s.e.m, n≥3, ***P<0.001, using a one-way ANOVA followed by Tukey's HSD test. Scale bar, 100 μm.

Supplementary Figure 7. Silencing CDH22 impairs hypoxic U87MG cell migration, invasion, and spheroid formation. (**A**) Western blot of CDH22 protein levels in control (Ctrl) cells stably expressing a non-targeting shRNA or in cells stably expressing one of two shRNAs targeting *CDH22* mRNA: Knockdown (KD) 3 and KD4. Two clones of each stable cell line were generated: KD3.1, KD3.2, KD4.1, and KD4.2. GAPDH used as a loading control. (**B**) Control and CDH22 KD cells exposed to normoxia (21% O_2) or hypoxia (1% O_2) for 24 h followed by wound generation. Representative images at 0 h (T0) and 12 h (T12) after wound generation. (**C-**

D) Transwell migration (**C**) and invasion (**D**) assays of control and CDH22 KD cells exposed to normoxia or hypoxia for 24 h. Representative images 12 h after seeding and stained with crystal violet. (**E**) Light micrographs of spheroids composed of control cells or CDH22-depleted cells (KD3.1). (**F-G**) Western blot of HIF-2α (**F**) and active caspase-3 (**G**) protein levels in lysates of spheroids composed of control cells or CDH22-depleted cells. Data are presented relative to normoxic Ctrl as mean ± s.e.m, n≥3, ***P<0.001, using a one-way ANOVA followed by Tukey's HSD test. Scale bar, 100 μm.

Supplementary Figure 8. Reintroduction of exogenous CDH22 restores the ability of U78MG cells to migrate, invade and adhere to one another in hypoxia. (**A**) Western blot of control (Ctrl) cells stably expressing a non-targeting shRNA, CDH22 knockdown control (KD Ctrl) cells stably expressing shRNA targeting *CDH22* mRNA and an exogenous empty vector or the *CDH22* codon-optimized coding sequence (clones Exo1 CDH22 and Exo2 CDH22) in hypoxia and normoxia. GAPDH used as a loading control. (**B-D**) Cells in **A** exposed to normoxia or hypoxia for 24 h followed by wound generation (**B**), or transwell migration (**C**) and invasion (**D**) assays. (**E**) Western blot of cells stably expressing shRNA targeting *eIF4E2* and either an empty vector (4E2KD Ctrl) or exogenous CDH22 (Exo CDH22). (**F-H**) Cells in **E** exposed to normoxia or hypoxia for 24 h followed by wound generation (**F**), or transwell migration (**G**) and invasion (**H**) assays. (**I-J**) Light micrographs of spheroids composed of CDH22-depleted (**I**) or eIF4E2-depleted (**J**) control cells expressing empty vector or exogenous CDH22. (**K-L**) Western blot of HIF-2α protein in lysates of spheroids from **I** (**K**) and **J** (**L**). (**M-N**) Spheroid migration assay (**M**) and 3D spheroid invasion assay (**N**) of spheroids composed of cells stably expressing exogenous CDH22. (**O**) Percent increase in spheroid area (invasion) in 3D invasion assay of

spheroids stably expressing exogenous CDH22 compared to controls stably expressing non-targeting shRNA. Data are presented as mean ± s.e.m, n≥3, ***P<0.001, using a one-way ANOVA followed by Tukey's HSD test. Scale bar, 100 μm.

Supplementary Figure 9. Proliferation and apoptosis rates of MDA-MB-231 and U87MG stable cells lines used in Figures 5, 6 and 8. (**A-B**) The proliferation rates measured by percent BrdU incorporation (**A**) and apoptosis rates measured by percent cells positive for active capsapse-3 (**B**) in normoxia (21% O_2) and hypoxia (1% O_2) of control (Ctrl) cells stably expressing a non-targeting shRNA, one of two shRNAs targeting *CDH22* mRNA: Knockdown (KD) 3 and KD4, and CDH22 knockdown control (KD Ctrl) cells stably expressing shRNA targeting *CDH22* mRNA and an exogenous empty vector or the *CDH22* codon-optimized coding sequence (Exo1 CDH22 and Exo2 CDH22). Data are presented as mean ± s.e.m of at least three biological replicates.

Supplementary Figure 1

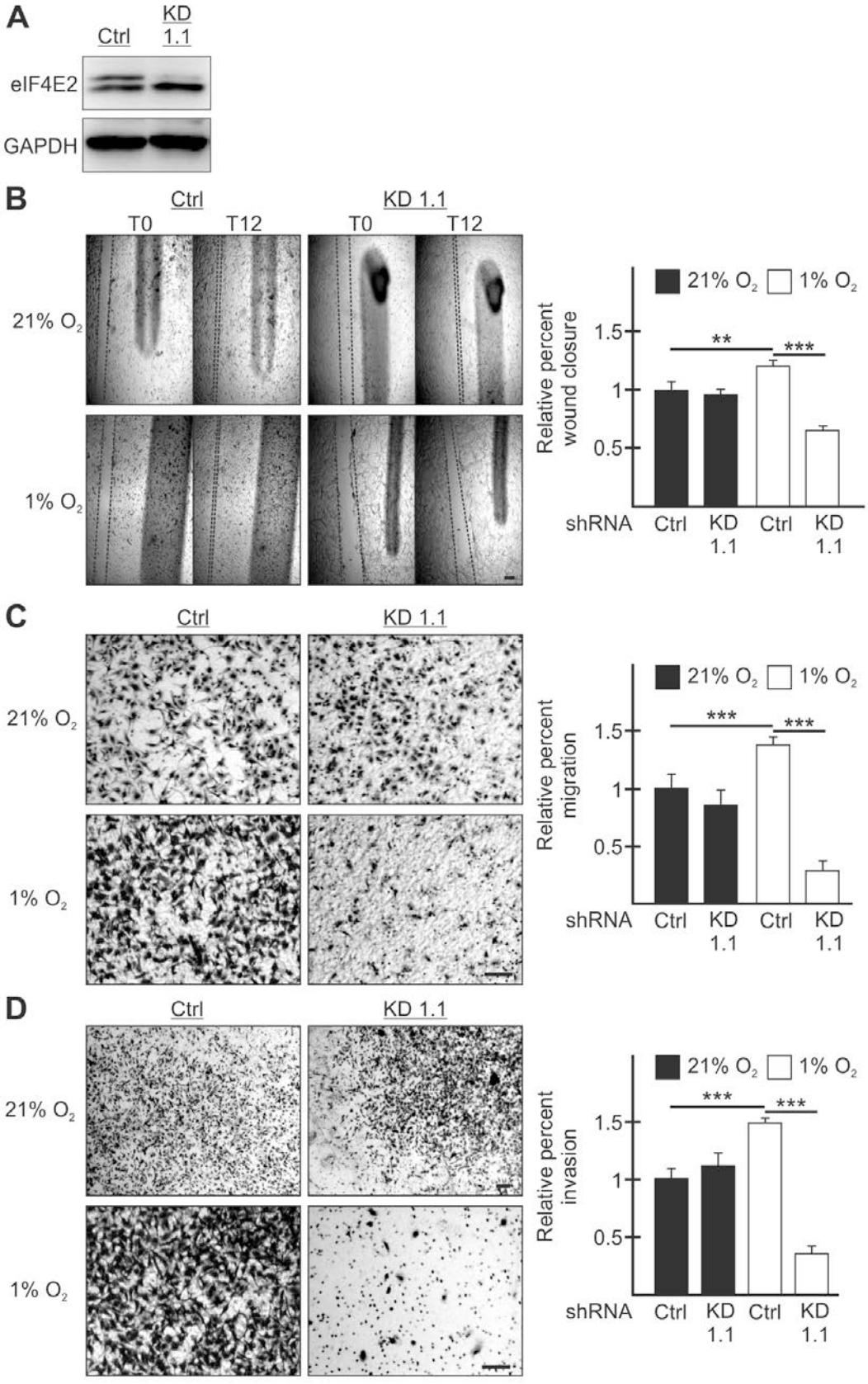

Supplementary Figure 2

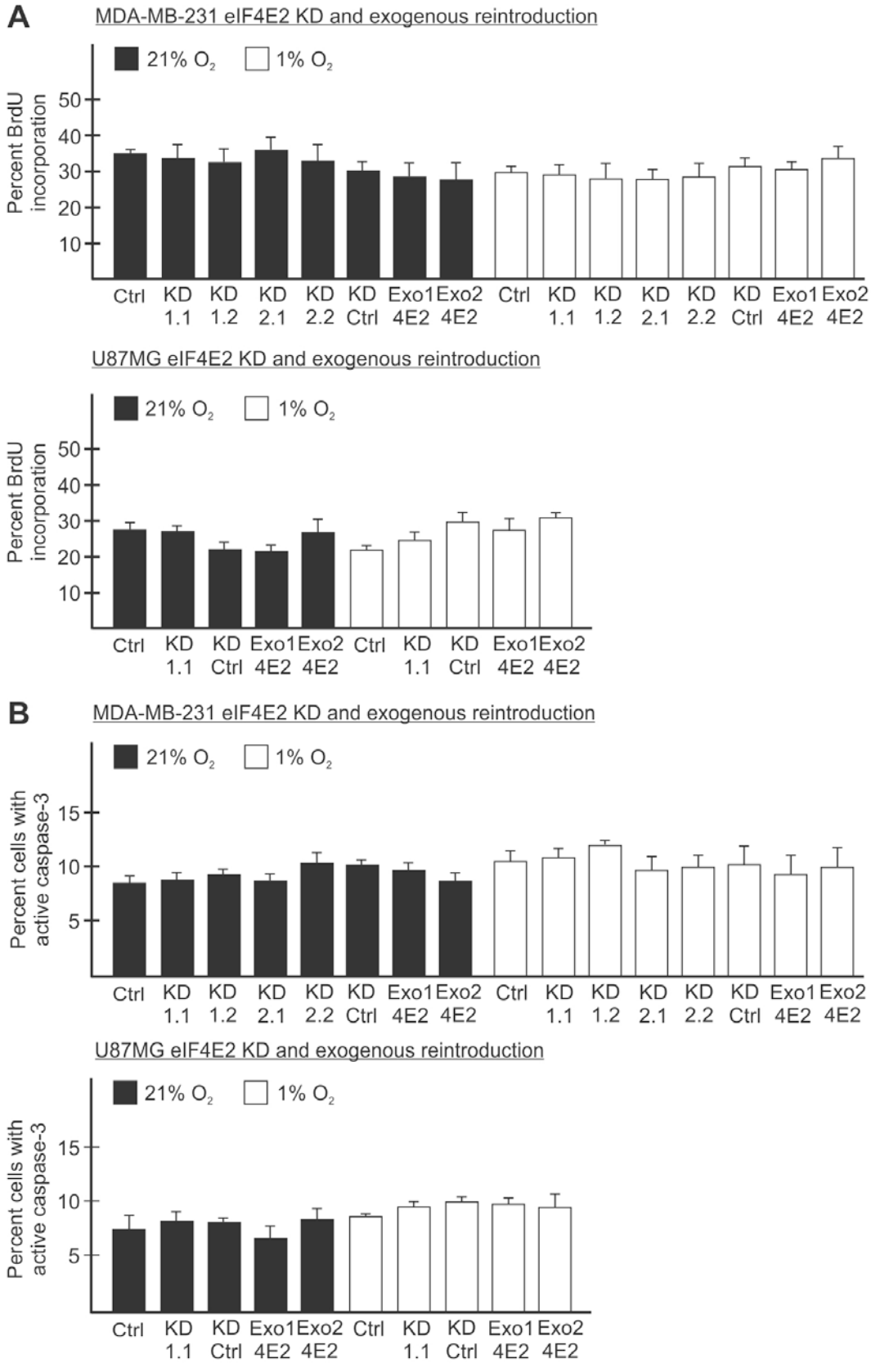

Supplementary Figure 3

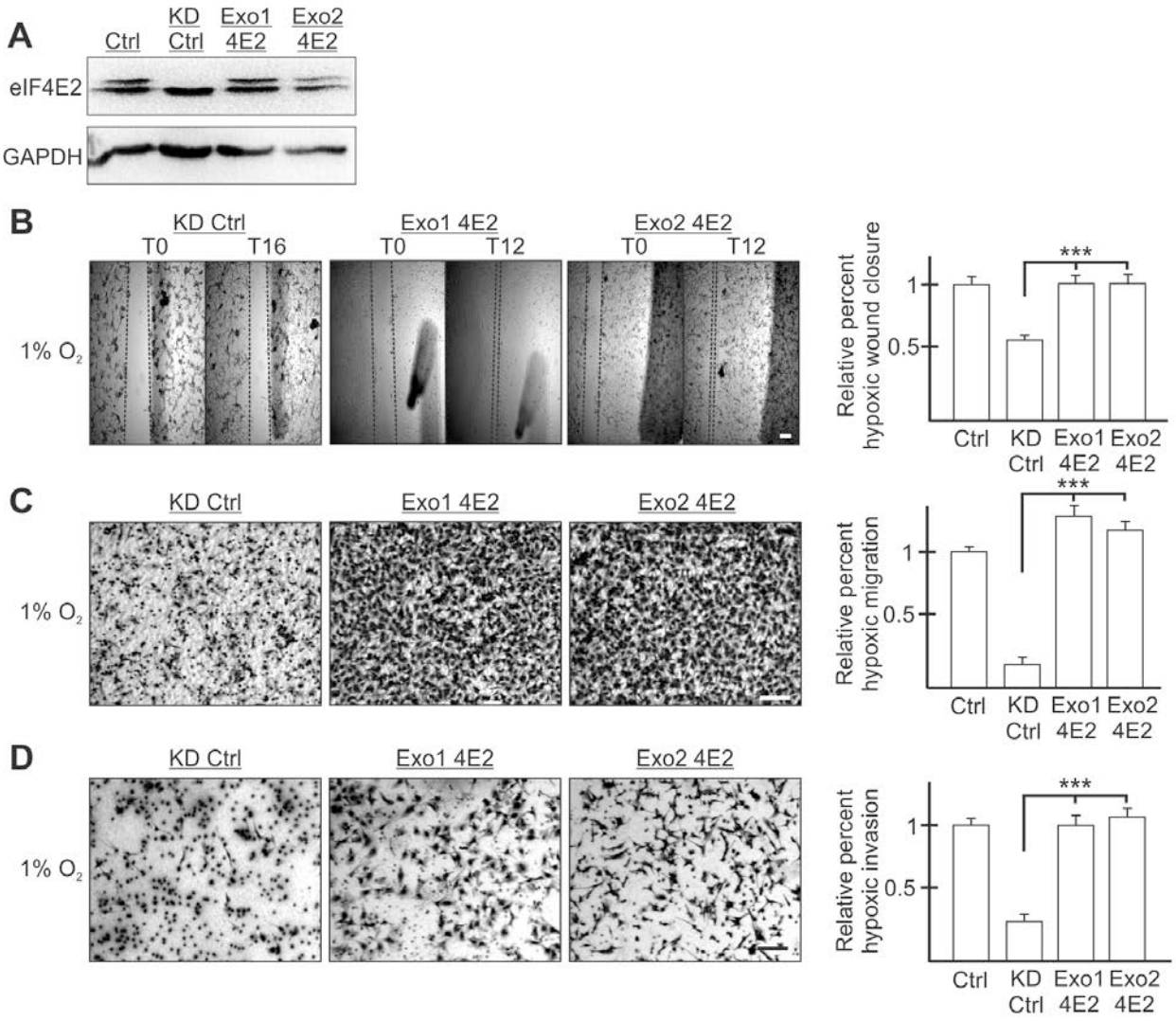

Supplementary Figure 4

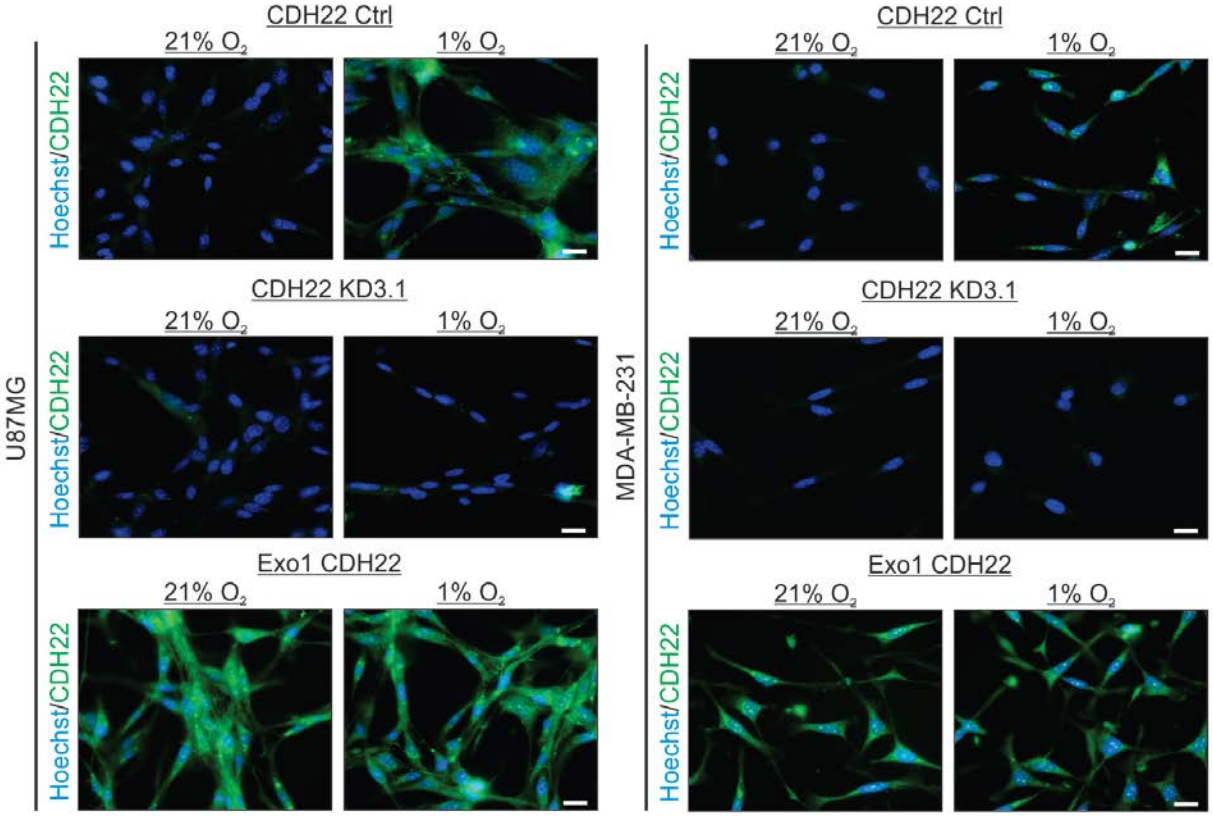

Supplementary Figure 5

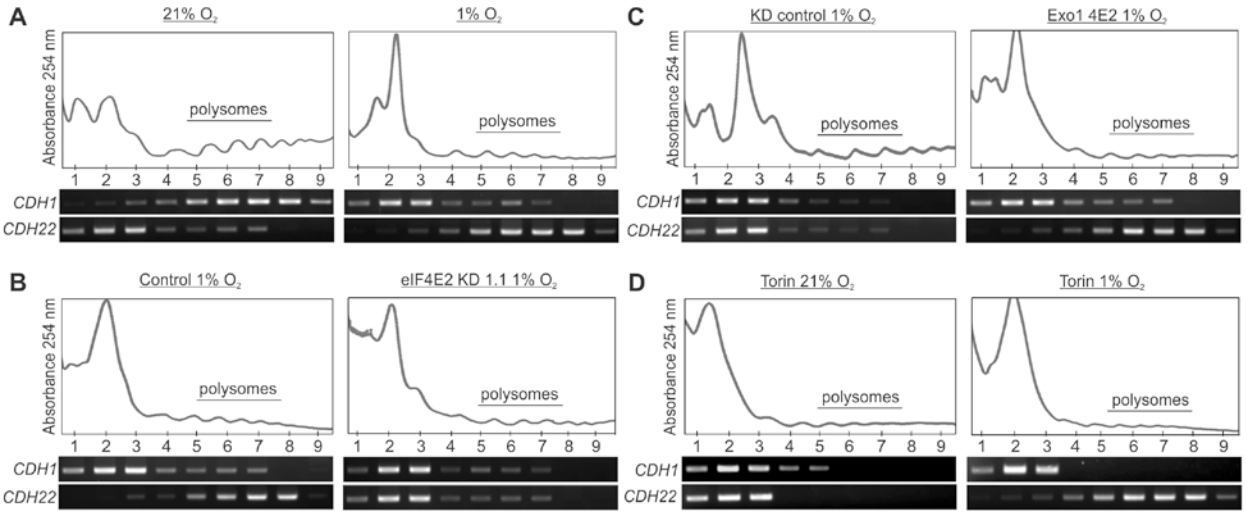

Supplementary Figure 6

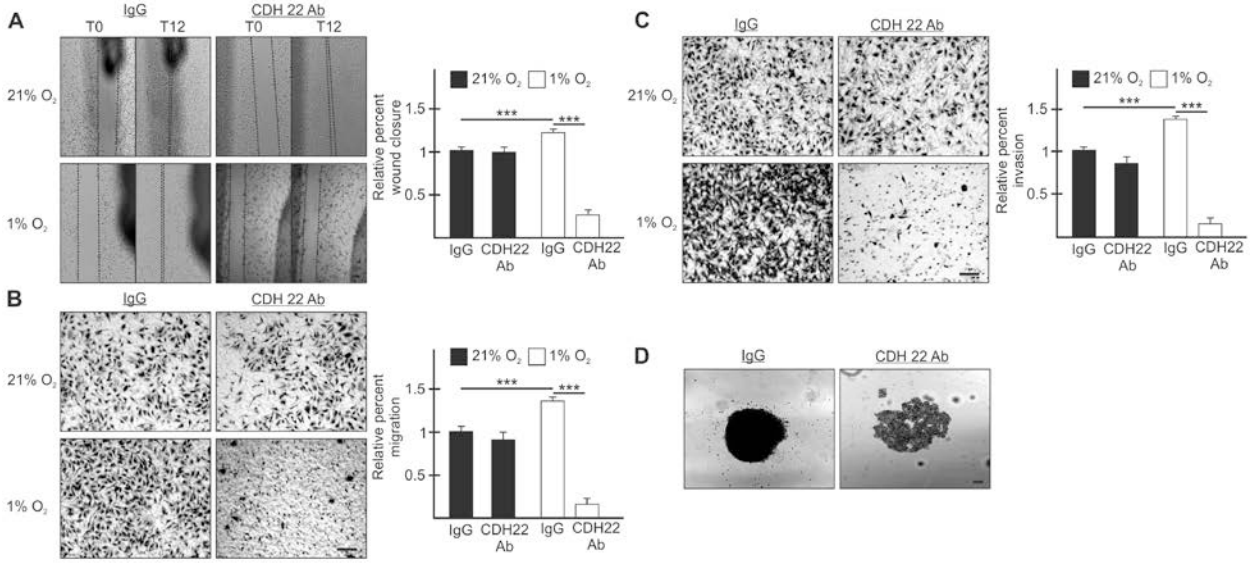

Supplementary Figure 7

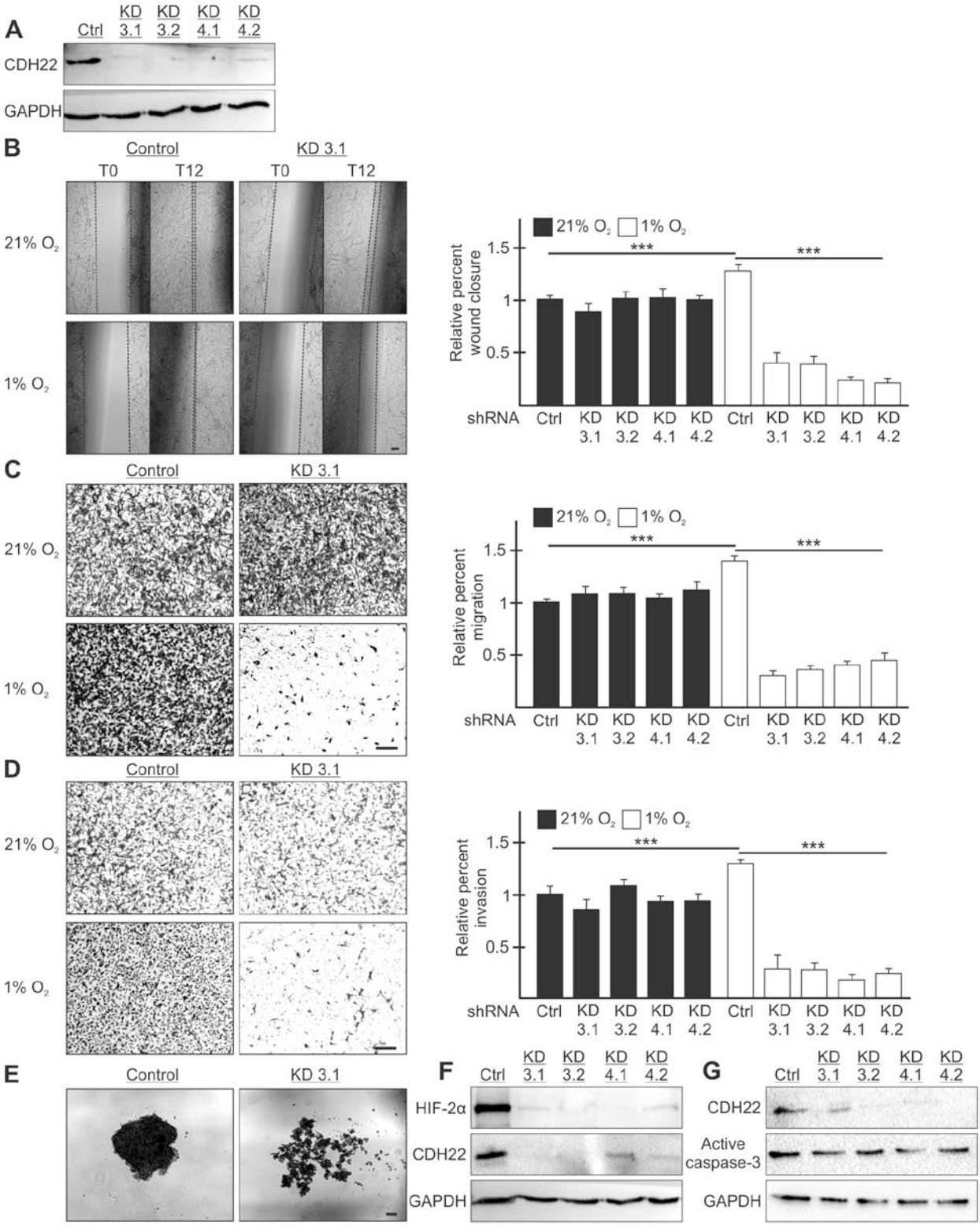

Supplementary Figure 8

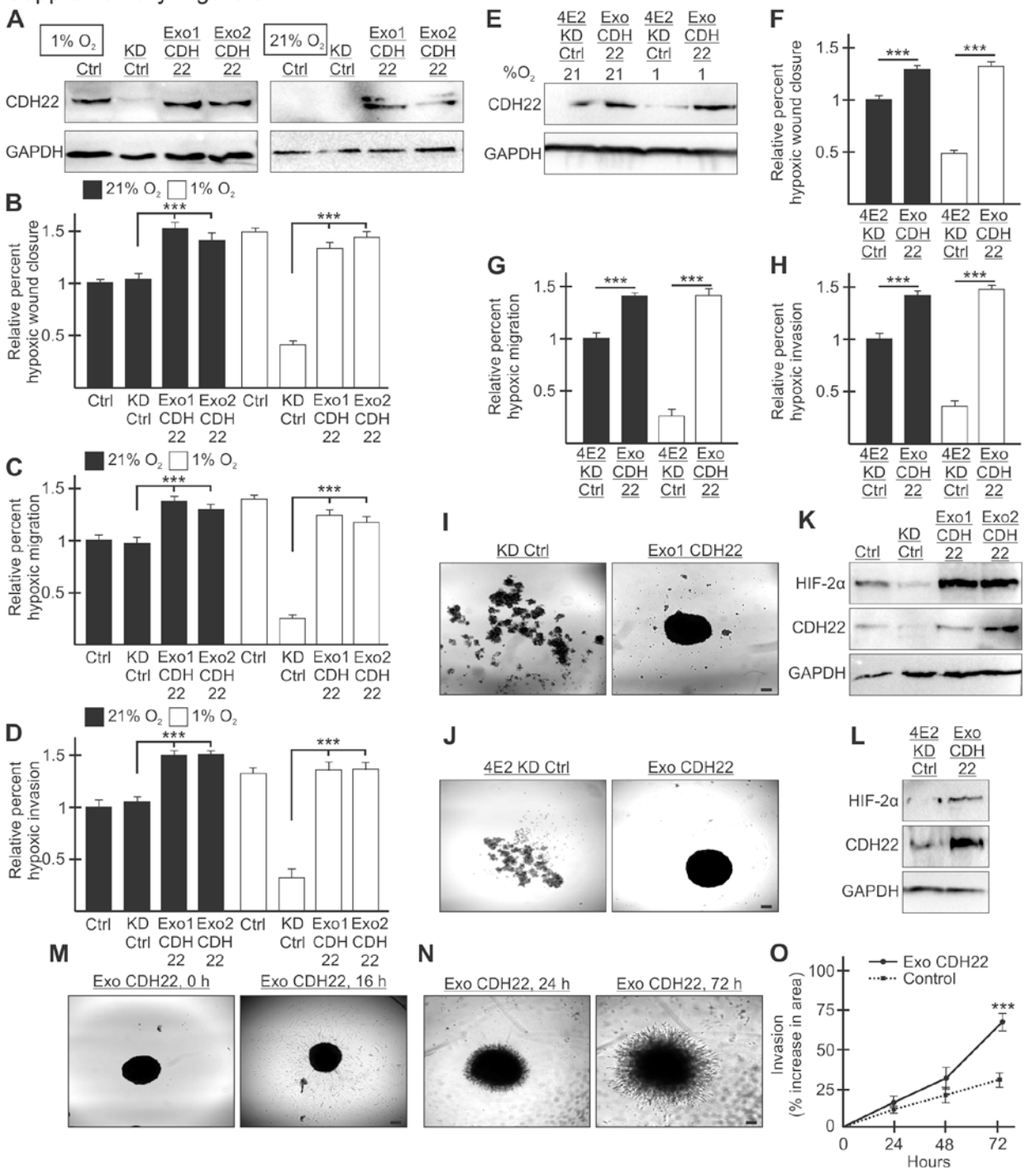

Supplementary Figure 9